Assimilation of ozone profiles from the Improved Limb Atmospheric Spectrometer-II: Study of Antarctic ozone

Ivanka Stajner,[1,2] Krzysztof Wargan,[1,2] Lang-Ping Chang,[1,2] Hiroo Hayashi,[1,3] Steven Pawson,[1] and Hideaki Nakajima[4]

Received 30 June 2005; revised 26 January 2006; accepted 28 March 2006; published 15 June 2006.

[1] Ozone data from the Improved Limb Atmospheric Spectrometer-II (ILAS-II) were included in addition to other satellite observations in the ozone assimilation system at the Global Modeling and Assimilation Office (GMAO) of NASA/Goddard. The control run assimilated data from NOAA 16 Solar Backscatter Ultraviolet/2 (SBUV/2) and Polar Ozone and Aerosol Measurement III (POAM III) instruments. Persistent impacts over Antarctica and transient impacts over northern middle and high latitudes are seen from April to October 2003, when ILAS-II provided good coverage. The largest improvements with respect to independent ozone sonde data are seen over the South Pole station. Ozone analyses and forecasts from the assimilation of SBUV/2, POAM III and ILAS-II data are used to investigate the transport of ozone to southern middle latitudes following the breakup of the Antarctic vortex. The quality of analyses and forecasts is evaluated by comparison with independent Stratospheric Aerosol and Gas Experiment III (SAGE III) ozone data near 46°S. Anomaly correlations between SAGE III data and forecasts are improved at 70 hPa when occultation data are included.

Citation: Stajner, I., K. Wargan, L.-P. Chang, H. Hayashi, S. Pawson, and H. Nakajima (2006), Assimilation of ozone profiles from the Improved Limb Atmospheric Spectrometer-II: Study of Antarctic ozone, *J. Geophys. Res.*, *111*, D11S14, doi:10.1029/2005JD006448.

1. Introduction

[2] The importance of ozone to terrestrial climate and ecosystems motivates a wide range of modeling and observational initiatives that aim to further our understanding of the processes that determine the time-dependent ozone distribution. Ozone data assimilation bridges the gap between models and observations, being a powerful technique for providing optimal estimates of the global ozone distribution using state-of-the-art models to interpolate the sometimes sparse observations to poorly observed regions. Ozone assimilation systems typically incorporate retrievals of daytime ozone obtained from measurements of backscattered solar irradiance [e.g., *Long et al.*, 1996; *Stajner et al.*, 2001; *Eskes et al.*, 2003; *Dethof and Hólm*, 2004]. Such measurements generally give good horizontal coverage, but rather coarse vertical resolution. Because of this intrinsic difficulty, ozone profiles in regions with high gradients, like the lower stratosphere, will be determined by the model. There is often much uncertainty in the assimilated products, especially in two regions which are important to the environment: near the polar night, where drastic ozone loss is possible, and below the ozone maximum, which is crucially important for climate forcing. This motivates including different types of data, determined from limb-sounding emission and occultation techniques.

[3] Solar occultation instruments provide accurate ozone profiles, with high vertical resolution (up to 1 km) down to cloud top, but these are spatially sparse with only about 15 profiles near a constant latitude in each hemisphere on any day [e.g., *Randall et al.*, 2003; *Brühl et al.*, 1996; *Wang et al.*, 2002; *Nakajima et al.*, 2006]. Assimilating these data presents a unique opportunity to benefit from their vertical information content, but a significant challenge because of their low horizontal density. Occultation data have thus typically not been assimilated, but have been used as high-quality validation data sets [e.g., *Stajner et al.*, 2001, 2004; *Wargan et al.*, 2005]. The potential value of occultation data in constraining assimilated fields in and around the Antarctic polar vortex has been shown by *Stajner and Wargan* [2004], who demonstrated positive impacts on the polar ozone profiles when Polar Ozone and Aerosol Measurement (POAM) III retrievals were added to the Solar Backscattered Ultraviolet/2 (SBUV/2) data in the NASA Goddard ozone data assimilation system.

[4] In the present paper we evaluate the impacts of assimilating Improved Limb Atmospheric Spectrometer-II (ILAS-II) ozone data in a similar system that already assimilates ozone data from SBUV/2 and POAM III instruments. The study is done over the Antarctic winter and spring 2003 when ILAS-II data were available. During this

[1] Global Modeling and Assimilation Office, NASA Goddard Space Flight Center, Greenbelt, Maryland, USA.
[2] Also at Science Applications International Corporation, Beltsville, Maryland, USA.
[3] Also at Goddard Earth Sciences and Technology Center, University of Maryland Baltimore County, Baltimore, Maryland, USA.
[4] National Institute for Environmental Studies, Tsukuba, Japan.

0148-0227/06/2005JD006448

period total ozone values reached lower levels than in any of the preceding 16 years at two stations in southern middle and high latitudes: Marambio (62°S) and Ushuaia (55°S) [*Pazmiño et al.*, 2005]. Given that ILAS-II and POAM III are both occultation instruments making measurements at nearby locations we ask the following questions: (1) Is there any additional impact from including ILAS-II data to the system that already assimilates SBUV/2 and POAM III data? (2) Does constraining ozone values in the Antarctic vortex through assimilation of POAM III and ILAS-II data help forecasting of ozone evolution in the southern middle latitudes following the vortex breakup?

2. Assimilation System

[5] Data assimilation provides a methodology for combining information from models and observations, according to their error characteristics, in order to provide optimal estimates of spatiotemporal distribution of geophysical fields [*Daley*, 1991]. The ozone assimilation system at NASA/Goddard [*Stajner et al.*, 2001] uses the sequential Physical-space Statistical Analysis System [*Cohn et al.*, 1998].

[6] The version of the ozone assimilation system used here is based on that described by [*Stajner et al.*, 2004] with the following enhancements. The ozone transport is implemented within the Goddard Earth Observing System version 4 (GEOS-4) general circulation model (GCM). The stratospheric gas-phase chemistry parameterization is based on the work of *Douglass et al.* [1996], with adjustments to ozone production rates in the upper stratosphere to reproduce an ozone climatology [cf. *Stajner et al.*, 2004]. The ozone assimilation remained univariate, and possible feedbacks of ozone into radiative calculations or infrared radiance assimilation were not used. All the meteorological variables other than ozone (e.g., temperature and winds) are taken from the Global Modeling and Assimilation Office (GMAO) operational analyses with the GEOS-4 system: GEOS-4.0.1 version from January to mid-May, followed by its GEOS-4.0.2 version to the end of the study period [*Bloom et al.*, 2005]. In these two versions stratospheric ozone transport is similar, and differences pertain to near surface temperature and humidity fields. The GCM includes flux-form semi-Lagrangian transport [*Lin and Rood*, 1996] at 1.25° longitude by 1° latitude resolution and 55 hybrid levels between the surface and 0.01 hPa.

3. Ozone Data

[7] In this study NOAA 16 SBUV/2 version 6 retrievals of total ozone columns and partial ozone columns in 5 km thick layers at pressures less than 64 hPa (Umkehr layers 4 to 12) are used [*Bhartia et al.*, 1996]. The nadir sounding geometry of the SBUV/2 instrument and the choice of measured wavelengths pose constraints on the vertical resolution of ozone retrievals. The physical principle of measurements of backscattered solar radiation limits the coverage to sunlit part of the globe, leaving polar night regions unobserved. Observation error specifications used in this study are taken from *Stajner et al.* [2001] for stratospheric partial columns and the standard deviations for the total columns are 2.5%.

[8] The ILAS-II instrument provided ozone profiles from solar occultation measurements in year 2003, with the best coverage from April to October [*Nakajima et al.*, 2006]. ILAS-II version 1.4 ozone profiles used in this study were validated by comparisons with ozone sondes and other satellite sensors: Halogen Occultation Experiment (HALOE), POAM III, Stratospheric Aerosol and Gas Experiment (SAGE) II and SAGE III [*Sugita et al.*, 2006]. On each day at most 15 ILAS-II profiles are retrieved in each hemisphere at nearly constant latitudes. Despite their sparseness the ILAS-II profiles are complementary to SBUV/2 because of their better vertical resolution (varying from ~1.5 to ~3 km) and poleward coverage during southern winter and spring. All ILAS-II ozone data were assimilated at retrieval locations, typically between the pressures of about 130 and 0.3 hPa, using random errors provided in the data files as observation errors.

[9] The POAM III instrument provides solar occultation profiles at almost identical latitudes as ILAS-II. Because of problems with the instrument during year 2003 the measurements were taken in only one hemisphere on each day, alternating between north and south on consecutive days. Following *Stajner and Wargan* [2004] we assimilated POAM III data between 14 and 60 km using specified observation errors of 5%. The current study uses recently released version 4 of POAM III data (J. Lumpe, personal communication, 2005). These retrievals include improved instrument pointing and altitude determination over the previous version 3 of POAM III data [*Lumpe et al.*, 2002; *Randall et al.*, 2003].

[10] Two sources of independent data are used for validation of results in this study: the South Pole ozone sondes [*Hofmann et al.*, 1997] and SAGE III ozone profiles [*Taha et al.*, 2004], which both provide high-quality, vertically resolved data in the lower and middle stratosphere. The South Pole station is typically within the core of the polar vortex, where substantial impacts are expected in the assimilation of ILAS-II and POAM III data. Following the breakup of the polar vortex we investigate the impact of ozone-depleted air on southern middle latitudes, which are observed by SAGE III occultation profiles at sunrise.

4. Impacts of ILAS-II Data

[11] The impacts of adding ILAS-II data to the assimilation that already uses SBUV/2 and POAM III data are shown in Figure 1. In the lower stratosphere at 70 hPa, the use of ILAS-II data increases ozone values in the core region of the polar vortex. A sustained impact is seen, ranging from ~2% in May, to ~5% in July, and finally to ~20% in September. Note the distinction between increased ozone in the vortex core region versus a slight decrease in the ozone toward the vortex boundary in September. The distinction between mixing properties of these two regions was pointed out by *Lee et al.* [2001]. In the middle stratosphere at 30 hPa, the assimilation of ILAS-II data reduces ozone over Antarctica. The largest impact of ~20% is seen in May, and it diminishes with time to ~10% in July and further to ~5% in September. The relative errors of ILAS-II data in the lower stratosphere increase with decreasing ozone values in September and October, and thus

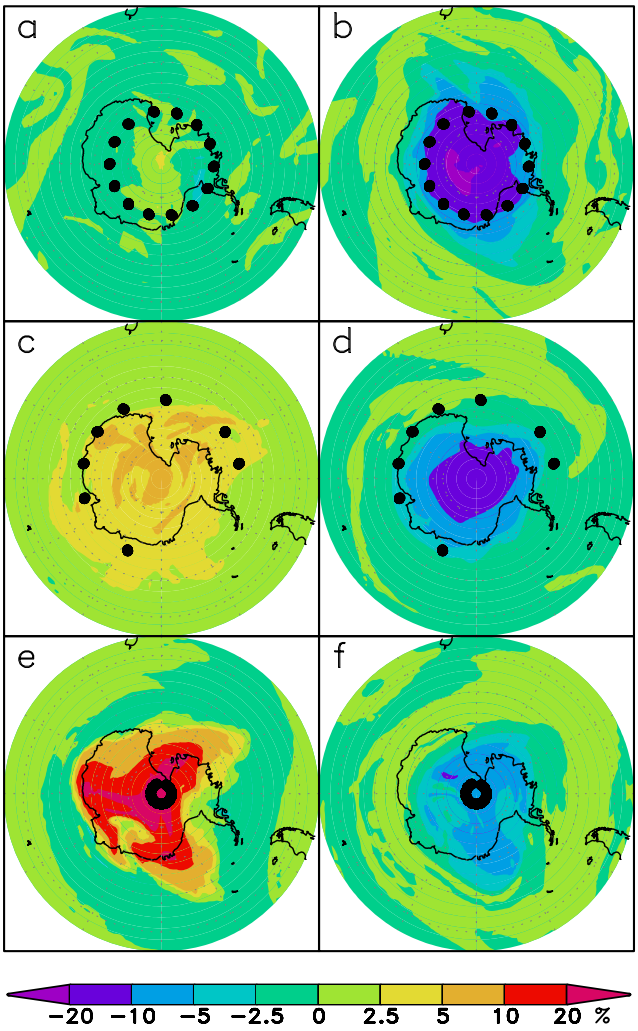

Figure 1. Maps of percentage differences between assimilation of SBUV/2, POAM III and ILAS-II data (SPI) and assimilation of SBUV/2 and POAM III data (SP). Percentage difference SPI-minus-SP is shown on (a and b) 1 May, (c and d) 10 July, and (e and f) 15 September at 70 hPa (Figures 1a, 1c, and 1e) and 30 hPa (Figures 1b, 1d, and 1f). Southern polar stereographic maps up to 45°S are used and the locations of ILAS-II data are marked by black circles.

the impact of ILAS-II data on the assimilated ozone is reduced in October.

[12] The ILAS-II data have a smaller impact in the summertime Northern Hemisphere that rarely exceeds 5%. The smaller impact is consistent with the larger relative errors reported for ILAS-II data there. Furthermore, different meteorological conditions between the two hemispheres lead to vastly different situations for these sparse data types. In the Antarctic, many of the occultation observations are located inside the polar vortex, which is dynamically isolated from the middle latitudes. This allows the impact of the occultation data to build up coherently inside the vortex, where there are no other observations to constrain the ozone distribution and compensate for model errors. For example, model tendencies excessively reduce zonal asymmetry in ozone, which will be discussed in Section 5 below. In the Northern Hemisphere, two effects are important. First, at and above the ozone maximum, the constraint by the abundant SBUV/2 data means that the ILAS-II data have a much smaller impact than in the polar night. Second, the absence of a mixing barrier in the summer means that air masses in the lower stratosphere that are subject to ILAS-II constraints are rapidly transported through middle and high latitudes and not persistently constrained as in the Antarctic. This highlights that the occultation data are most useful when applied repeatedly to the same subset of air masses, as occurs in the isolated polar vortex throughout the winter.

[13] The largest impact of ILAS-II data is seen near the South Pole, whether ILAS-II measurements were close to it as in September or further away as in July. Independent ozone sonde profiles at the South Pole are used in evaluation of the quality of assimilation runs (Figure 2). On 10 July the assimilation that used SBUV/2 and POAM III data overestimates the ozone between 30 and 40 hPa and underestimates the ozone near 70 hPa. The assimilation that includes additional data from the ILAS-II instrument typically has lower ozone values around 30 hPa and higher ozone values near 70 hPa. Both of these changes improve the agreement between the assimilated ozone and the ozone sonde profile. Similar impacts were seen in most comparisons with the ozone sondes at the South Pole in June and July. In October the assimilation of SBUV/2 and POAM III data already agrees well with the ozone sonde profile, and the addition of ILAS-II data has a very small impact. As expected, the addition of POAM III and ILAS-II occultation data to the assimilation that uses only SBUV/2 (not shown) improves Antarctic ozone profiles in winter and spring, resembling the enhancements seen from assimilation of POAM III data by *Stajner and Wargan* [2004].

[14] Specific impacts of ILAS-II data can be attributed to differences between ILAS-II and POAM III instrument coverage, error specifications that were used in the assimilation of their data, and to the retrieved ozone values, each of which is now discussed in turn.

[15] During the period studied here the POAM III instrument experienced difficulties in regular operation. Instead of observing both hemispheres on each day, POAM III made measurements in only one hemisphere on each day, alternating between north and south. Consequently, the amount of POAM III data is about a half of those that were available in 1998 and used by *Stajner and Wargan* [2004], while ILAS-II provides relatively uniform coverage in both hemispheres daily.

[16] We use observation errors of 5% for POAM III data in the assimilation experiments, following *Stajner and Wargan* [2004]. Error estimates included in the ILAS-II data files were used in the assimilation of ILAS-II data in order to help in validation of not only ILAS-II ozone, but also of the error estimates. There is a strong time dependence in the relative error estimates for ILAS-II ozone. At 70 hPa they increase from about 15% for the period between April and September (Figure 3a) to more than 50% in October (Figure 3b). Consequently the impact of ILAS-II data diminishes in October, but a substantial improvement was seen at the South Pole in July (recall Figure 2). One possibility is that the improved profile shape could be due to the use of additional ILAS-II data with relatively low errors. However, ILAS-II observation errors

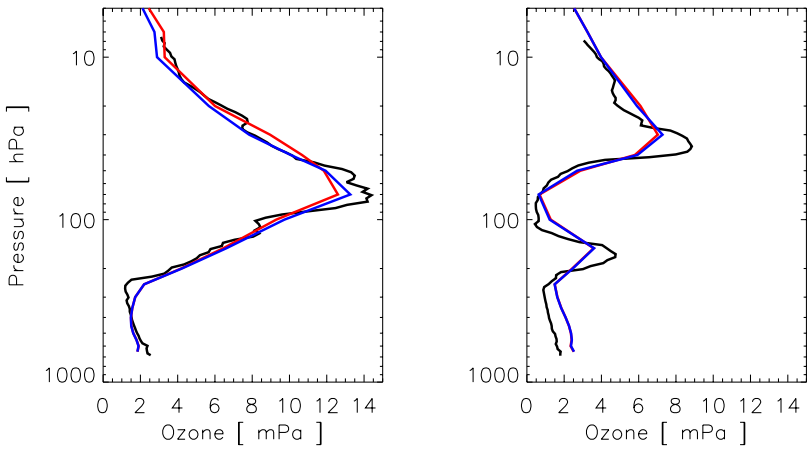

Figure 2. Comparisons of ozone sonde profiles at the South Pole (black) on (left) 10 July 2003 and (right) 31 October 2003 with collocated profiles from SP analyses (red) and SPI analyses (blue).

are lower than those for POAM III only in the layer between 2 and 20 hPa (Figure 4).

[17] Differences in the retrieved ozone values from the two occultation instruments are indicated by monthly mean differences between either ILAS-II or POAM III and short-term model forecasts, i.e., observed-minus-forecast (O-F) residuals in Figure 4. ILAS-II O-F residuals tend to be smaller on average than POAM III O-F residuals in two layers: for pressure up to 5 hPa and 20–50 hPa. Near 7–10 hPa the O-F residuals for two occultation data sets agree well. Our findings are consistent with the comparisons of ozone values from these two occultation data sets by *Sugita et al.* [2006]. In addition, our comparisons indicate that average ILAS-II O-F residuals near 70 hPa change from smaller than POAM III O-F residuals in April, over O-F residuals very similar to those of POAM III in May and June, to O-F residuals larger than those of POAM III in July to September, which is in agreement with the impacts of ILAS-II assimilation seen in Figure 1. In October SBUV/2 observations are constraining the assimilated ozone over Antarctica and O-F residuals for ILAS-II and POAM III increase in magnitude, with a negative peak around 5 hPa, and a positive peak around 30 hPa. Qualitatively similar behavior, but with negative peak around 20 hPa and positive peak around 70 hPa, is seen in the Northern Hemisphere throughout the duration of our experiments (not shown). Good coverage of SBUV/2 data near ILAS-II and POAM III locations is common to October in the Southern Hemisphere and April-October in the Northern Hemisphere. The large excursions of O-F residuals, are consistent with known biases in the SBUV/2 data relative to occultation data. For example, SAGE II data are lower (higher) than SBUV/2 data in the layer 16–32 hPa (32–64 hPa) in the northern middle latitudes, and SAGE II data are higher than SBUV/2 data in the layer 16–32 hPa in the southern middle latitudes [*McPeters et al.*, 1994].

[18] The ILAS-II ozone data have a substantial impact on the assimilated fields over Antarctica of up to 20% (Figure 1), which improves the profile shape and the agreement with the South Pole ozone sondes (Figure 2). This impact is consistent with the fact that ILAS-II retrieved values are often lower than those from POAM III, and agrees with the differences between ILAS-II and POAM III O-F residuals, which show variability with altitude and

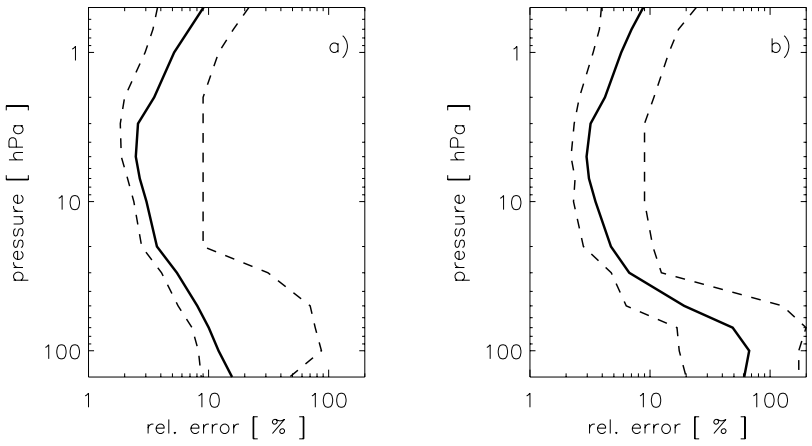

Figure 3. Average (solid) and range (dashed) of ILAS-II error estimates for all the profiles in the Southern Hemisphere in (a) June and (b) October 2003.

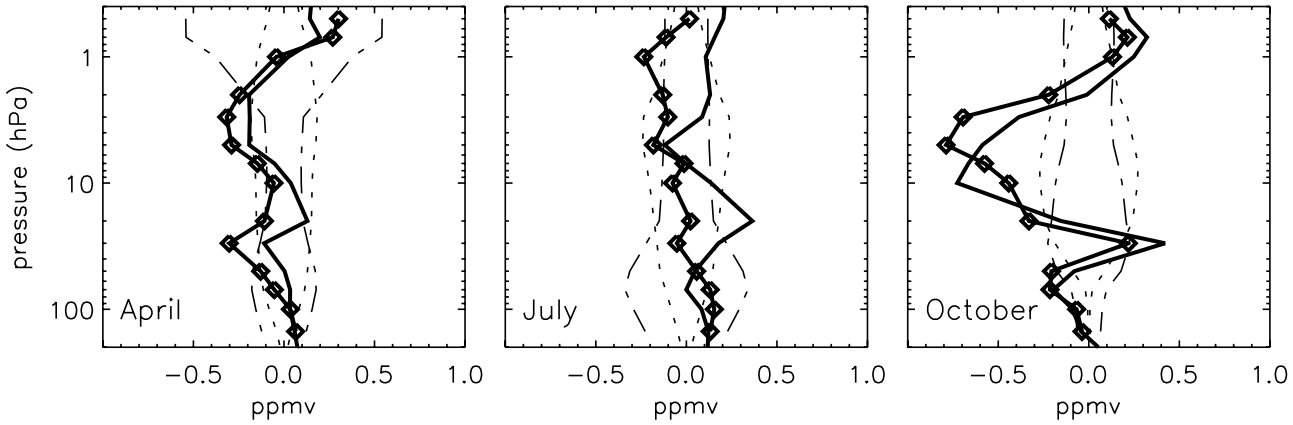

Figure 4. Monthly mean observed-minus-forecast (O-F) residuals are shown for ILAS-II (solid line with diamonds) and POAM III data (solid line). Mean errors used for assimilation of ILAS-II (dot-dashed) and POAM III data (dotted) are shown for comparison. All means are computed for data that were first binned into pressure layers bounded by 0.3, 0.5, 0.7, 1, 2, 3, 5, 7, 10, 20, 30, 50, 70, 100, and 150 hPa.

time. The ILAS-II O-F residuals do not deviate much from ILAS-II error estimates, except when biases in SBUV/2 data affect the analyses.

5. Ozone Evolution Over Antarctica

[19] Monthly mean fields from SBUV/2, POAM III and ILAS-II assimilation describe qualitatively the evolution of lower stratospheric temperature and ozone during Antarctic spring. Mean fields for September are shown in Figure 5 (top). The Antarctic vortex (marked by lowest temperatures) shows a hint of the zonal wave number three that was prominent on some days (e.g., 15 September, Figure 1e). There is also a shift of the vortex toward 45°W, which induces zonal wave number one in temperature and ozone fields. The ozone depletion that starts at the vortex edge does not fully advance toward the South Pole in the September average yielding ring-like shape of the lowest ozone. Model tendencies attempt to make the ozone field more zonal by increasing ozone east of the dateline and decreasing ozone east of the Greenwich meridian. In contrast, the analysis increments of the opposite sign are trying to strengthen zonal asymmetry in ozone. The average temperature field in October (Figure 5, bottom) shows that the vortex is shifted toward 45°E. Ozone within the vortex is fully depleted. The analysis increments are similar to those seen in September. However, the model tendencies are dominated by the dynamical events at the end of October. The elongation of the vortex at the end of October roughly in the direction of the 60–240°E and the squeezing of the vortex in the orthogonal direction causes the largest positive model tendencies. Ozone rich air from outside the vortex displaces ozone-depleted air from within the vortex (see positive model tendencies near 150°E).

[20] This example shows how assimilation of sparse occultation data helps to provide a coherent picture of the ozone evolution in the Antarctic polar stratosphere. Note that the assimilation of SBUV-only data misses two important features of ozone evolution over Antarctica: wintertime accumulation of ozone in the lower stratosphere and vertical confinement of the springtime ozone loss [*Stajner and Wargan*, 2004]. The assimilating model supplies accompanying temperature fields, dynamical and chemical tendencies. Together with data induced analysis increments they provide a comprehensive description of the ozone evolution during winter and spring.

6. Ozone Forecasts in Springtime

[21] The elongation of the vortex that started in late October intensified in November, as the vortex broke up in a manner typical of the Southern Hemisphere [e.g., *Lahoz et al.*, 1996], leading to vortex breakup and transport of ozone-depleted air from the vortex core into southern middle latitudes. The ozone distribution around the vortex is determined by horizontal advection and diabatic descent [*Pierce et al.*, 1993]. For example, the ozone analysis at 30 hPa on 5 November shows low-ozone air stretching along 120°E from Antarctica to middle latitudes (Figure 6). Note also high ozone gradients very close to the South Pole.

[22] The vertical structure of the elongated ozone feature on 5 November is illustrated by a longitude-pressure section at 50°S on 5 November (Figure 7). This reveals a westward slope (with increasing altitude) of the low-ozone feature, with the corresponding higher ozone values from outside the polar vortex on its eastern flank. Temperature contours illustrate the correspondence of this ozone feature with the occurrence of a baroclinic zone. This is dynamically similar to those examined during warming events in the 1984–1985 northern winter by *Fairlie et al.* [1990]. Figure 7 shows that the baroclinic feature is quite deep, extending between about 70 hPa and 20 hPa. This complex dynamics together with high gradients in ozone that were set up by previous chemical processes make early November an interesting period for a study of the evolution of ozone in southern middle latitudes.

[23] During early November 2003, SAGE III measurements are available near 46°S. In order to evaluate the

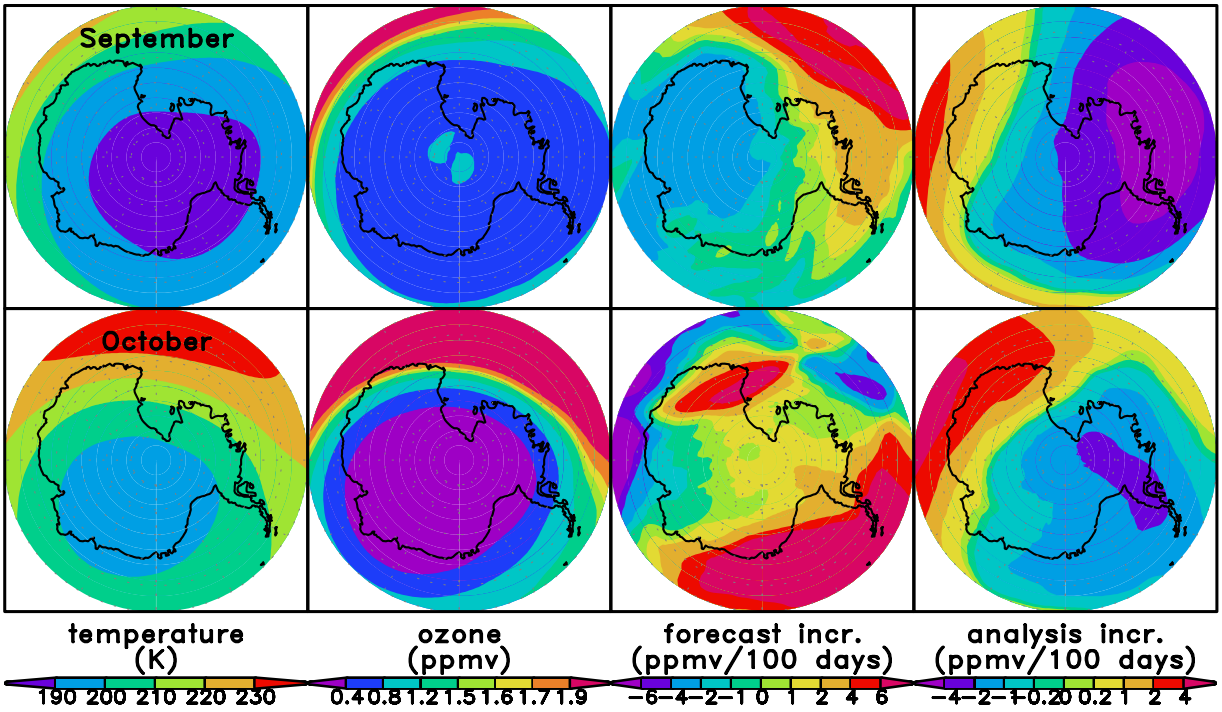

Figure 5. Mean fields at 70 hPa for (top) September and (bottom) October 2003. The fields are temperature (K) (first column), ozone (ppmv) (second column), changes to the ozone due to forecast model (one hundredths of one ppmv per day) (third column), and ozone analysis increments (one hundredths of one ppmv per day) (fourth column). These are south polar stereographic maps for the region poleward of 60°S with Greenwich meridian at the bottom of each map.

realism of the ozone analyses and forecasts, longitude-time series (Hovmoeller plots) near 46°S are compared with SAGE III data. SAGE III data are binned to the nearest 10° longitude and plotted using colored squares over the underlying analysis or forecast field, using an identical color scale (Figure 8). The most prominent feature in the time series at 30 hPa is the low ozone starting near 60°E on 1 November, with an accompanying high ozone near 90°E (Figure 8a). This feature travels eastward as it diminishes in strength, disappearing by around 10 November. SAGE III measurements near this feature confirm the realism of both low and high ozone values and their eastward propagation. Note that away from this feature the ambient midlatitudinal air has not been constrained by ILAS-II or POAM III data, but only by SBUV/2 data, and the ozone concentrations are lower than the SAGE III values. The comparison of SAGE III with the forecast that was started on 30 October at 1800 UT shows similarly good agreement, with somewhat less low-ozone air passing through around 5 November (Figure 8c) and a hint of a reduced ozone bias in the ambient midlatitudinal air.

[24] At 70 hPa the agreement between SAGE III and analyses in the depth and the breadth of the low ozone around 90°E on 3 November (Figure 8b) is quite good. The regions with depleted ozone are transported realistically in the analyses. However, there are some clear discrepancies in the ozone forecast (Figure 8d). The low-ozone feature in the forecast seen near 60°E on 8 November advanced too far east in comparison with both analyses and SAGE III data. Note also the ozone low-passing near the dateline in the

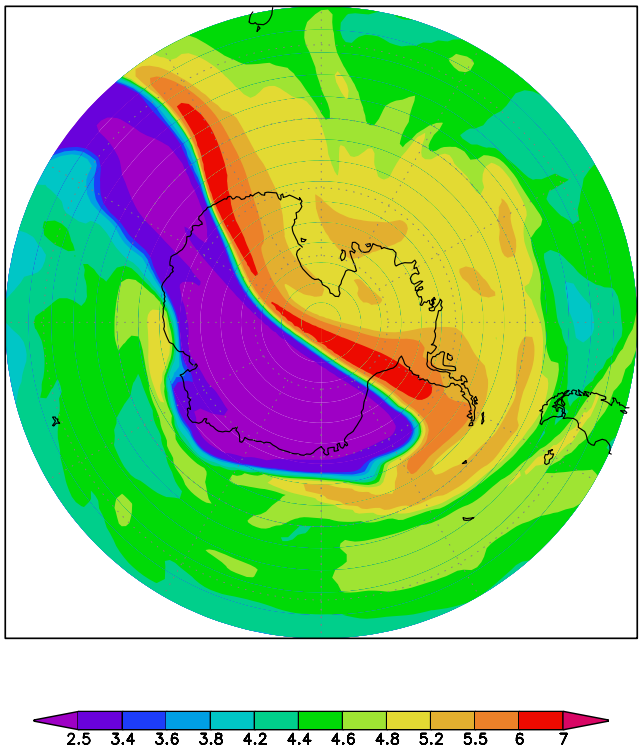

Figure 6. Ozone field (ppmv) at 30 hPa at 1200 UT on 5 November shown in the south polar stereographic projection poleward of 45°S.

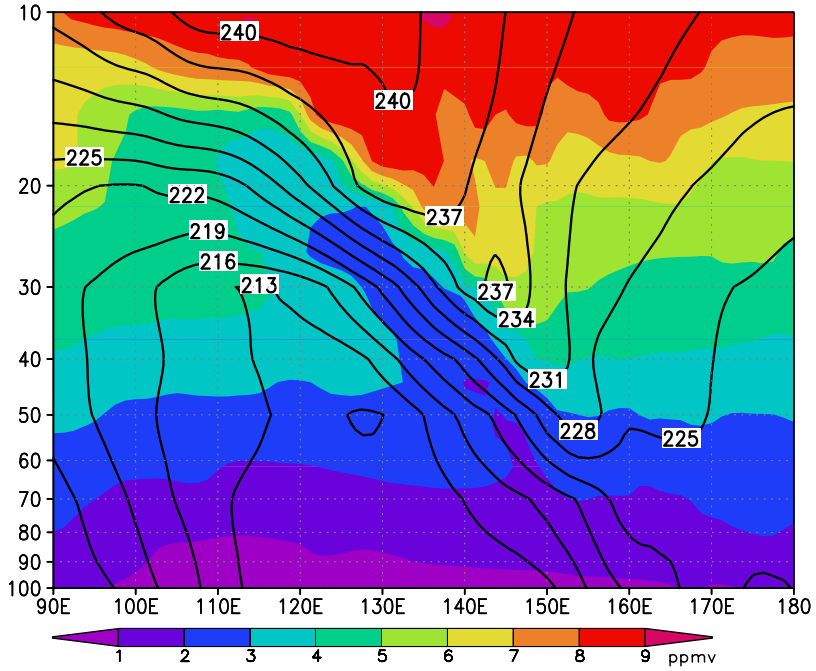

Figure 7. Longitude-pressure section at 50°S, between 90°E and the date line and 100–10 hPa, on 5 November 2003. The shading shows the analyzed ozone distribution (color scale with increments of 1 ppmv), and the contours show analyzed temperature (contour interval 3 K).

analyses on 14 November, which agrees well with the SAGE III data (Figure 8b). The SAGE III measurement near 120°E on 4 November confirm the baroclinic nature of the fields shown in Figure 7): in the same profile the ozone is atypically high at 30 hPa (red square in Figure 8a) and atypically low at 70 hPa (Figure 8b). Qualitative comparison of features in the analyses and forecasts with SAGE III ozone shows that they are captured quite realistically, with indication of some biases in the analyses and with excessive eastward propagation due to the dynamical developments in the forecasts.

[25] A quantitative measure of the forecast quality is provided by anomaly correlations, which are commonly used for forecast verification in the numerical weather prediction (NWP) [e.g., *Wilks*, 1995]. For the period 1–10 November, time series of the anomalies (i.e., values minus their spatial and temporal mean) were constructed for the SAGE III data and the analyses and forecasts sampled at the SAGE III locations. Correlations were computed between these anomalies as a function of the forecast length, with analyzed values corresponding to forecast length zero. To aid interpretation, similar anomaly correlations were computed for time series of three other pairs of data: (1) forecasts from SBUV/2-only analyses against SAGE III data; (2) the forecasts from SBUV/2-POAM-ILAS analyses against their own analyses, in the traditional NWP usage; and (3) for persistence, where analyses valid n days before SAGE III measurements (n = 0, 1, . . ., 10) are compared against the SAGE III data, similar to *Eskes et al.* [2002]. The time series of these anomaly correlations at 70 and 30 hPa in Figure 9 reveal a number of properties.

[26] 1. Comparing the solid and dashed lines in Figure 9 reveals the extent to which the occultation data impact the forecast skill in relation to the SAGE III data. At 70 hPa the analyses that included occultation data show improved forecast skill due to a better constraint on the small air mass advected from high latitudes. At 30 hPa the impact of POAM III and ILAS-II data on the forecast skill is negligible: prior to reaching 46°S the low-ozone air in analyses was constrained by SBUV/2 data, which effectively removes the impact of ILAS-II and POAM III data on ozone in middle latitudes. This is consistent with findings of *Stajner and Wargan* [2004] that the impact of POAM data in springtime is strong over the South Pole, decreases toward the edge of Antarctica and further into middle latitudes, at levels where SBUV provides good data.

[27] 2. The skill for persistence (dash-dotted lines in Figure 9) are shown to help quantify what a meaningful forecast skill may be. The skill for persistence at 30 and 70 hPa drops off quickly to about 0.2 in 3–4 days. Model forecasts have skill higher than persistence for up to 7 days at 30 hPa and for up to 9 days at 70 hPa.

[28] 3. The traditional measure of forecast skill (dashed line with circles in Figure 9) illustrates two points. First, validation against the analysis means the curve starts with a value of unity at time zero, decaying as the forecast states diverge from the analyses as time moves on. These anomaly correlations decay to about 0.8 at 4 days and 0.6 after about 6 days at both levels. Second, the values at day zero in these calculations give a measure of disagreement between the analyses and the independent SAGE III data. The analyses are constrained by version 6 of SBUV/2 data, which are known to be about 10% lower than SAGE II data in the Umkehr layer 5 (15–32 hPa) in the southern middle latitudes (30–50°S) [*McPeters et al.*, 1994]. At 70 hPa the anomaly correlations against SAGE III data (solid line)

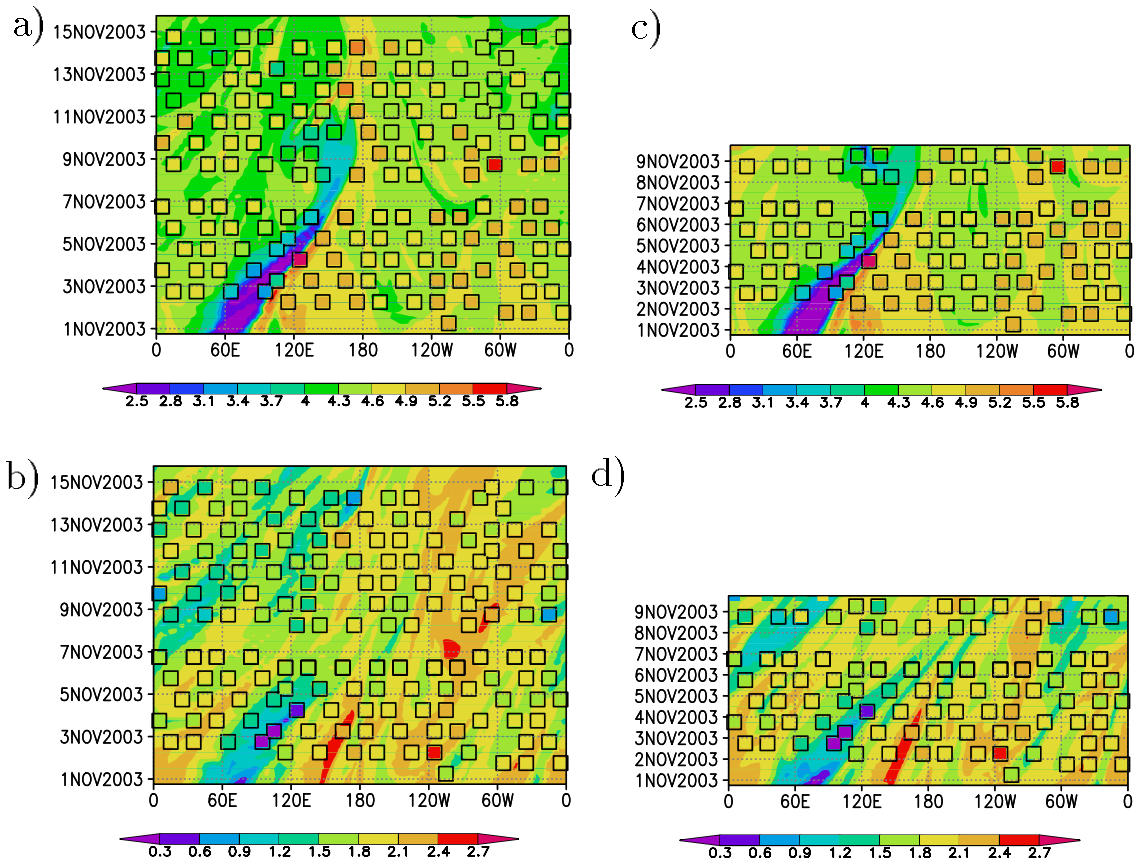

Figure 8. Ozone (ppmv) time series comparison for 1–15 November of SAGE III and analyses at 46°S at (a) 30 hPa and (b) 70 hPa. Comparison of SAGE III and ozone forecast started on 30 October at 1800 UT at (c) 30 hPa and (d) 70 hPa. Time range for forecast time series is 1–9 November (Figures 8c and 8d). SAGE values are plotted in squares using the same color scale as in the underlying analysis or forecast fields.

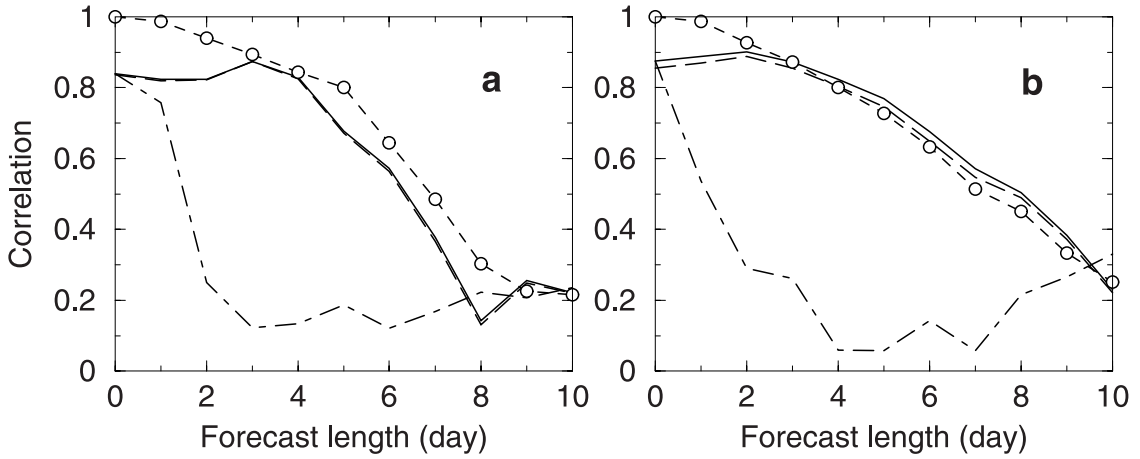

Figure 9. Anomaly correlations between SAGE III and collocated ozone forecasts as a function of forecast length started from the analyses of POAM III, ILAS-II and SBUV/2 data (solid curve). Same is shown for forecasts started from SBUV/2-only assimilation (dashed) and for persistence (dot-dashed). In each case, forecast time zero corresponds to the analysis. Anomaly correlations of forecasts from analyses of POAM III, ILAS-II and SBUV/2 data against those analyses at 46°S are shown (dashed with circles). (a) At 30 hPa and (b) at 70 hPa.

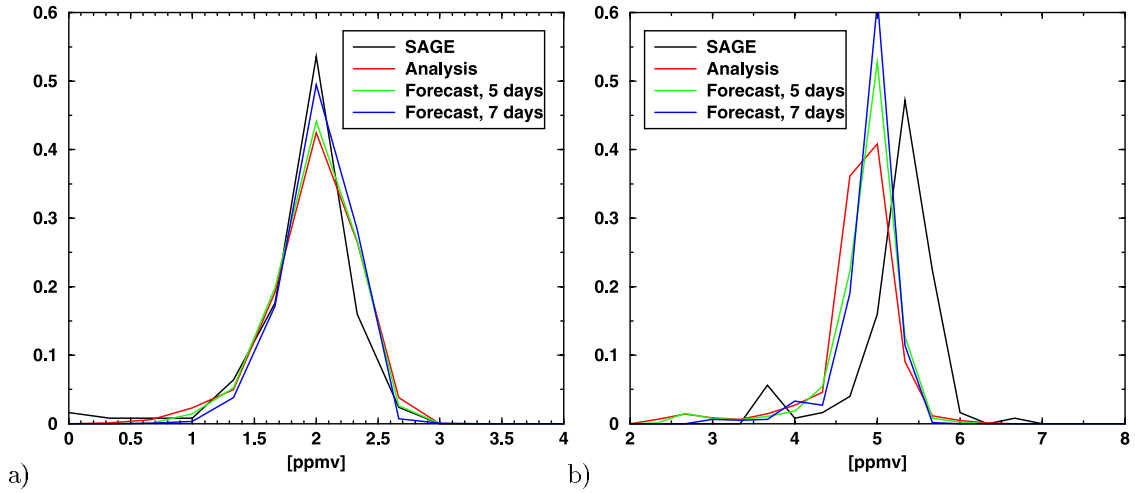

Figure 10. Normalized histograms of SAGE III ozone (black), analyses (red), 5-day forecasts (green) and 7-day forecasts (blue) at 46°S for 1–10 November at (a) 70 hPa and (b) 30 hPa.

remain above 0.8 for 4 days, and fall below 0.6 on day 7. At 30 hPa there is an initial increase in the anomaly correlations from 0.84 for analyses to 0.87 for the 3-day forecasts. Within the first 3 days the forecasts drift away from the analyses. The increase in the mean field brings it closer to SAGE III mean and improves the baseline for computation of anomaly correlations. The curves for validation against own analyses and against SAGE III converge over these first forecast days, then decay in parallel at both levels. However, at 30 hPa the bias between SBUV/2 and SAGE III data persists through the forecast, with the dashed curve crossing any value of anomaly correlation almost a day later than the solid curve. At 70 hPa the positive impact of the occultation datasets are apparent throughout the forecasts, with better anomaly correlations against the SAGE III data than against the system's own analyses.

[29] A study spanning several winters is needed to examine how robust these results are. Nevertheless, we found anomaly correlations exceeding 0.6 for 5–6 days at 30, 50 and 70 hPa in southern middle latitudes following the vortex breakup in November 2003 using SAGE III data for verification.

[30] Representation of constituent data using their probability distribution function (PDF) provides another view of the data that may help in characterizing their basic statistical properties, as well as contributions of different transport regimes [e.g., *Sparling*, 2000]. The PDFs for all the SAGE III sunrise data in 0.33-ppmv-wide bins for 1–10 November at 70 or 30 hPa are shown in Figure 10. They are compared with PDFs of all model data at 46°S at the same level during 1–10 November. Note that data from all 288 model grid points 1.25° longitude apart at all four synoptic times per day are used. Three instances of the model fields are used: analyses, 5-day forecasts and 7-day forecasts. At 70 hPa SAGE III data have a stronger mode at 2 ppmv than the analyses (Figure 10a). With an advancing forecast length the mode becomes more pronounced at the expense of underrepresenting lower (1.3 ppmv) or higher (2.66 ppmv) values. Both analyses and forecasts have too many points in the 2.3 ppmv bin compared to SAGE III. Nevertheless, means of analyses and SAGE III distributions are not different at a 0.01 level of significance.

[31] At 30 hPa SAGE III data show three peaks in the distribution (Figure 10b). Most of the air has midlatitudinal values (close to the mode at 5.33 ppmv). Lower values around 3.66 ppmv are suggestive of air that was previously within the vortex core. A possible pathway for the air with higher values around 6.66 ppmv is that it originated in the tropics, traveled poleward, possibly even descending near the vortex edge, then being advected back into middle latitudes during vortex breakup. In the analyses, the mode is shifted a bin lower than in SAGE III, indicating the low bias in the analyses. Forecasts have an increasingly stronger mode with advancing forecast length, meaning the ozone field becomes more uniform as the forecasts advance, possibly because of stronger barriers to meridional transport. The 7-day forecasts do not capture the very low ozone values of 2.6 ppmv, which are represented in the analyses and 5-day forecasts. Note that the spatial sampling of SAGE III poses limitations for interpretation of the low-ozone air that is crossing 46°S around 60°E on 1 November (Figure 8a). In the analyses this feature spans only about 30° of longitude and SAGE III measures near its edges, never quite seeing the region where the analyses have their lowest values. The largest difference between the PDFs for the 3-day forecast (not shown) and the analyses is the shift of values from the 4.66- to the 5-ppmv bins, which increases the mean of the forecast and brings it closer to SAGE III. This supports the possible explanation of the increase in the anomaly correlations due to the bias reduction that was mentioned in the discussion of Figure 9.

[32] Some of the loss in the forecast skill is manifested as spatial misalignment between the low- or high-ozone features in the forecast flow and verification data. For example, a 5-day forecast for 5 November at 30 hPa is shown in Figure 11a. Compared to the ozone analysis at the same time (Figure 6), the forecast field suggests an excessively barotropic, solid-body like rotation. More pronounced symmetry in the forecast than in the analyzed ozone is consistent with an average zonal wind that is more than 5 m/s

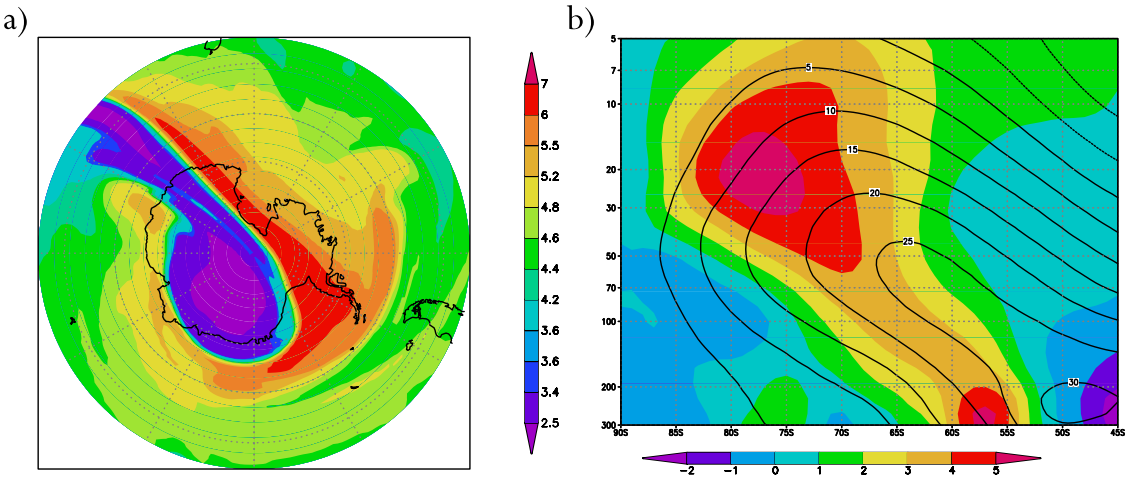

Figure 11. (a) Five-day ozone forecast (ppmv) at 30 hPa for 5 November at 1200 UT shown (compare analysis in Figure 6). (b) Average analysis zonal wind (m/s) for 1–10 November (contour) and the average difference between 5-day wind forecast and analysis (color) shown for 90–45°S and 300–5 hPa.

stronger in the forecasts than in the analyses near 30 hPa and 75°S (Figure 11b), and with fewer low ozone values in the middle latitudes due to a stronger mixing barrier at high latitudes (Figure 10b).

7. Conclusions

[33] This study uses solar occultation data from two instruments, ILAS-II and POAM III, together with data from the nadir-viewing NOAA 16 SBUV/2 instrument within a global ozone assimilation system. Substantial impacts of ILAS-II data are found within the Antarctic vortex in the year 2003 (Figure 1). The use of ILAS-II data improves the comparison of ozone analyses with the South Pole ozone sonde in the winter (Figure 2). A study of ozone evolution in the southern middle latitudes following the breakup of the Antarctic vortex reveals realistic representation of ozone variability in the analyses (Figures 6 and 7). This is followed by qualitative and quantitative comparisons of analyses and forecasts against independent SAGE III data near 46°S (Figures 8–10). Anomaly correlations exceed 0.6 for up to 5–7 days in the middle and lower stratosphere (30, 50 and 70 hPa). The loss in the forecast skill with advanced forecast length seems to be related to a stronger zonal wind (Figure 11b) that could pose a barrier to transport of low-ozone air to middle latitudes (Figure 10b) and possibly also cause an eastward shift in flow features (Figure 11a).

[34] The evolution of ozone at two levels is investigated. At 70 hPa there is a large dynamic range of values due to an ozone accumulation in wintertime, and a full depletion in the spring inside the "ozone hole." At 30 hPa near the top of the "ozone hole" the ozone loss is more subtle (Figure 2). ILAS-II ozone is typically lower than POAM III ozone at 30 hPa, and ILAS-II ozone is typically higher than POAM III ozone at 70 hPa in the Southern Hemisphere between April and August. Note that we initially used version 3 of POAM III data, and our comparisons indicate that version 4 of POAM III data is more consistent with ILAS-II data.

[35] The evolution of low-ozone air masses is of interest for estimation of surface UV radiation [*Pazmiño et al.*, 2005]. Assimilation of occultation data into an ozone model provides a way of estimating ozone within the vortex, and the forecasting capability allows predictions of the evolution of the low-ozone air as it enters middle latitudes in the springtime. The value of occultation data for surface UV forecasts over South America using assimilation of ozone data into a three-dimensional model could be evaluated in a future study.

[36] The analyses successfully propagate the information from the Antarctic vortex into middle latitudes in November. The forecasts are relatively successful in predicting ozone variability, but show somewhat excessive eastward transport and vortex persistence, which also poses a barrier to transport of air away from the pole. The dynamical nature of errors in the ozone forecasts raises another possibility. If occultation data were available even a day or two after measurements were taken, they could be assimilated into a three-dimensional model to provide an initial condition with a realistic representation of the Antarctic vortex. The model could be then integrated using analyzed meteorological fields up to the real time. The use of analyzed meteorology would allow more accurate representation of the dynamics during this past period. A day or two long forecast issued from the present time would likely still contain the information from previous occultation data and would not suffer from the accumulation of dynamical errors seen in the longer forecasts. This option may be investigated in the future.

[37] The use of occultation data is critical for the success of this study. When only SBUV/2 data are assimilated ozone depletion at 70 hPa inside the vortex is not fully captured. Consequently the transport of that air to middle latitudes does not decrease the ozone to the values seen by the SAGE III instrument. This demonstrates the value for assimilation of data from space based occultation instruments such as POAM III and ILAS-II, whose orbits facilitate repeated observations within the Antarctic vortex.

The assimilation of such occultation data improves the qualitative and quantitative agreement with independent measurements (from sondes and SAGE III) and provides opportunities for the further study of the impacts of ozone-depleted vortex air on the southern middle latitudes in springtime. It is planned to compare the impacts of these occultation data with those of limb-emission data (e.g., MIPAS assimilation [*Wargan et al.*, 2005]), which have the advantage of better spatial coverage but generally have less vertical resolution and lower precision. A potential advantage of occultation data is that the unified record of such observations spans several years, compared to the shorter periods observed with limb-emission measurements, making them better suited for study of interannual variations in polar ozone and its dispersion into middle latitudes.

[38] **Acknowledgments.** This work was supported by NASA's Atmospheric Chemistry and Modeling Program grant 622-55-61. The ILAS-II data that were used in this study were obtained from the ILAS-II instrument developed by the Ministry of the Environment of Japan on board the ADEOS-II that was launched by the NASDA. The data were processed at the ILAS-II Data Handling Facility, National Institute for Environmental Studies.

References

Bhartia, P. K., R. D. McPeters, C. L. Mateer, L. E. Flynn, and C. Wellemeyer (1996), Algorithm for the estimation of vertical ozone profile from the backscattered ultraviolet (BUV) technique, *J. Geophys. Res.*, *101*, 18,793–18,806.

Bloom, S. C., et al. (2005), The Goddard Earth Observing System Data Assimilation System, GEOS DAS version 4.0.3: Documentation and validation, *Tech. Rep. Ser. on Global Model. and Data Assimilation 104606*, *26*, 181 pp., NASA Goddard Space Flight Cent., Greenbelt, Md.

Brühl, C., et al. (1996), HALOE ozone channel validation, *J. Geophys. Res.*, *101*, 10,217–10,240.

Cohn, S. E., A. da Silva, J. Guo, M. Sienkiewicz, and D. Lamich (1998), Assessing the effects of data selection with the DAO Physical-Space Statistical Analysis System, *Mon. Weather Rev.*, *126*, 2913–2926.

Daley, R. (1991), *Atmospheric Data Analysis*, Cambridge Univ. Press, New York.

Dethof, A., and E. V. Hólm (2004), Ozone assimilation in the ERA-40 reanalysis project, *Q. J. R. Meteorol. Soc.*, *130*, 2851–2872.

Douglass, A., C. Weaver, R. Rood, and L. Coy (1996), A three-dimensional simulation of the ozone annual cycle using winds from a data assimilation system, *J. Geophys. Res.*, *101*(D1), 1463–1474.

Eskes, H., P. van Velthoven, and H. Kelder (2002), Global ozone forecasting based on ERS-2 GOME observations, *Atmos. Chem. Phys.*, *2*, 271–278.

Eskes, H. J., P. F. J. van Velthoven, P. J. M. Valks, and H. M. Kelder (2003), Assimilation of GOME total ozone satellite observations in a three-dimensional tracer transport model, *Q. J. R. Meteorol. Soc.*, *129*, 1663–1681.

Fairlie, T. D. A., M. Fisher, and A. O'Neill (1990), The development of narrow baroclinic zones and other small-scale structure during simulated major warmings, *Q. J. R. Meteorol. Soc.*, *116*, 287–315.

Hofmann, D. J., S. J. Oltmans, J. M. Harris, B. J. Johnson, and J. A. Lathrop (1997), Ten years of ozonesonde measurements at the South Pole: Implications for recovery of springtime Antarctic ozone, *J. Geophys. Res.*, *102*(D7), 8931–8944.

Lahoz, W. A., A. O'Neill, A. Heaps, V. D. Pope, R. Swinbank, R. S. Harwood, L. Froidevaux, W. G. Read, J. W. Waters, and G. E. Peckham (1996), Vortexdynamics and the evolution of water vapour in the stratosphere of the Southern Hemisphere, *Q. J. R. Meteorol. Soc.*, *122*, 423–450.

Lee, A., H. Roscoe, A. Jones, P. Haynes, E. Shuckburgh, M. Morrey, and H. Pumphrey (2001), The impact of the mixing properties within the Antarctic stratospheric vortex on ozone loss in spring, *J. Geophys. Res.*, *106*(D3), 3203–3212.

Lin, S.-J., and R. B. Rood (1996), Multidimensionsl flux-form semi-Langrangian transport schemes, *Mon. Weather Rev.*, *124*, 2046–2070.

Long, C. S., A. J. Miller, H.-T. Lee, J. D. Wild, R. C. Przywarty, and D. Hufford (1996), Ultraviolet index forecasts issued by the National Weather Service, *Bull. Am. Meteorol. Soc.*, *77*, 729–748.

Lumpe, J. D., R. M. Bevilacqua, K. W. Hoppel, and C. E. Randall (2002), POAM III retrieval algorithm and error analysis, *J. Geophys. Res.*, *107*(D21), 4575, doi:10.1029/2002JD002137.

McPeters, R. D., T. Miles, L. E. Flynn, C. G. Wellemeyer, and J. M. Zawodny (1994), Comparison of SBUV and SAGE II ozone profiles: Implication for ozone trends, *J. Geophys. Res.*, *99*(D10), 20,513–20,524.

Nakajima, H., et al. (2006), Characteristics and performance of the Improved Limb Atmospheric Spectrometer-II (ILAS-II) on board the ADEOS-II satellite, *J. Geophys. Res.*, doi:10.1029/2005JD006334, in press.

Pazmiño, A. F., S. Godin-Beekmann, M. Ginzburg, S. Bekki, A. Hauchecorne, R. D. Piacentini, and E. J. Quel (2005), Impact of Antarctic polar vortex occurrences on total ozone and UVB radiation at southern Argentinean and Antarctic stations during 1997–2003 period, *J. Geophys. Res.*, *110*, D03103, doi:10.1029/2004JD005304.

Pierce, R. B., W. T. Blackshear, T. D. Fairlie, W. L. Grose, and R. E. Turner (1993), The interaction of radiative and dynamical processes during a simulated sudden stratospheric warming, *J. Atmos. Sci.*, *50*, 3829–3851.

Randall, C. E., et al. (2003), Validation of POAM III ozone: Comparisons with ozonesonde and satellite data, *J. Geophys. Res.*, *108*(D12), 4367, doi:10.1029/2002JD002944.

Sparling, L. C. (2000), Statistical perspectives on stratospheric transport, *Rev. Geophys.*, *38*(3), 417–436.

Stajner, I., and K. Wargan (2004), Antarctic stratospheric ozone from the assimilation of occultation data, *Geophys. Res. Lett.*, *31*, L18108, doi:10.1029/2004GL020846.

Stajner, I., L. P. Riishøjgaard, and R. B. Rood (2001), The GEOS ozone data assimilation system: Specification of error statistics, *Q. J. R. Meteorol.Soc.*, *127*, 1069–1094.

Stajner, I., N. Winslow, R. B. Rood, and S. Pawson (2004), Monitoring of observation errors in the assimilation of satellite ozone data, *J. Geophys. Res.*, *109*, D06309 doi:10.1029/2003JD004118.

Sugita, T., et al. (2006), Ozone profiles in the high-latitude stratosphere and lower mesosphere measured by the Improved Limb Atmospheric Spectrometer (ILAS)-II: Comparison with other satellite sensors and ozonesondes, *J. Geophys. Res.*, *111*, D11S02, doi:10.1029/2005JD006439.

Taha, G., L. W. Thomason, C. R. Trepte, and W. P. Chu (2004), Validation of SAGE III Data Products version 3.0, paper presented at XX Quadrennial Ozone Symposium, Int. Ozone Comm., Athens, Greece.

Wang, H. J., D. M. Cunnold, L. W. Thomason, J. M. Zawodny, and G. E. Bodeker (2002), Assessment of SAGE version 6.1 ozone data quality, *J. Geophys. Res.*, *107*(D23), 4691, doi:10.1029/2002JD002418.

Wargan, K., I. Stajner, S. Pawson, R. B. Rood, and W.-W. Tan (2005), Monitoring and assimilation of ozone data from the Michelson Interferometer for Passive Atmospheric Sounding, *Q. J. R. Meteorol. Soc.*, *131*, 2713–2734, doi:10.1256/qj.04.184.

Wilks, D. S. (1995), *Statistical Methods in the Atmospheric Sciences. An Introduction*, 467 pp., Elsevier, New York.

L.-P. Chang, H. Hayashi, S. Pawson, I. Stajner, and K. Wargan, Global Modeling and Assimilation Office, Code 610.1, NASA Goddard Space Flight Center, Greenbelt, MD 20771, USA. (lpchang@gmao.gsfc.nasa.gov; hhayashi@gmao.gsfc.nasa.gov; spawson@gmao.gsfc.nasa.gov; istajner@gmao.gsfc.nasa.gov; kwargan@gmao.gsfc.nasa.gov)

H. Nakajima, National Institute for Environmental Studies, Tsukuba 305-8506, Japan.